Photodetachment Imaging Studies of the Electron Affinity of CF_3

Hans-Jürgen Deyerl, Leah S. Alconcel, and Robert E. Continetti*

Department of Chemistry and Biochemistry, University of California, San Diego, 9500 Gilman Drive, La Jolla, California 92093-0314

Received: August 30, 2000; In Final Form: November 15, 2000

The photoelectron spectra of the trifluoromethyl anion, CF_3^-, at 355 and 258 nm are reported. Simulation of the partially resolved vibrational structure is used to extract the adiabatic electron affinity, AEA[CF_3] = 1.82 ± 0.05 eV. The heat of formation for the trifluoromethyl anion derived from the adiabatic electron affinity ($\Delta H^0_{f,298}[CF_3^-] = -153.4 \pm 1.5$ kcal/mol) is compared to the high-accuracy "isodesmic bond additivity corrected" (BAC) complete basis set (CBS-Q) theory prediction ($\Delta H^0_{f,298}[CF_3^-] = -152.6$ kcal/mol). We find the CBS-Q prediction of $\Delta H^0_{f,298}[CF_3] = -112.1$ kcal/mol, after BAC, to be in excellent agreement with the most recent experimental determination of the radical heat of formation. The photoelectron angular distribution at 355 nm was also extracted from the photoelectron image, revealing p wave photodetachment with an energy-averaged anisotropy parameter of $\beta = 1.5 \pm 0.1$.

1. Introduction

Photoelectron spectroscopy, in conjunction with high level ab initio calculations, has proven to be a powerful method for the determination of thermochemical data and structural parameters of reactive intermediates,[1] such as free radicals,[2,3] carbenes,[4] and negative ions.[5,6] The trifluoromethyl radical (CF_3) and its corresponding ions are known to be important intermediates in high-energy environments such as the upper atmosphere[7] and in halocarbon plasmas used for etching of semiconductors.[8] For modeling processes in these environments, accurate thermochemical data on the reacting species are required. Due to uncertainties in the thermochemistry of both CF_3 and CF_3^-, studies of the energetics and dynamics of these molecules are of continued interest.[9,10] One important quantity, the adiabatic electron affinity (AEA) of CF_3, is still in question. The empirical data for AEA [CF_3] spans the range from 1.7 to 3.3 eV.[11−13] Collective consideration of the values in this set and their sources clearly places AEA[CF_3] in the 1.7−2.5 eV range, with a probable value below 2.0 eV; yet no experiments have been performed with a stated uncertainty less than 0.16 eV.

The $^2A_1$ ground state of CF_3 has been previously studied spectroscopically. In an electron-spin-resonance (ESR) study, Fessenden et al.[14] found a nonplanar structure for CF_3. Matrix-isolation studies of CF_3 by Jacox and co-workers[15] determined the vibrational frequencies in C_{3v} symmetry. Gas-phase vibrational frequencies were assigned by Carlson et al.[16] in a flash photolysis experiment and by Bozlee et al.[17] by coherent anti-Stokes Raman spectroscopy (CARS). Infrared diode laser spectroscopy was also applied for an accurate determination of the geometry.[18] Recently, Ahser and Ruscic[19] remeasured by photoionization mass spectrometry the CF_3^+ fragment ion yield curves from C_2F_4 and reported a heat of formation of $\Delta H^0_{f,298}[CF_3] = -111.4 \pm 0.9$ kcal/mol and an adiabatic ionization potential of IP[CF_3] = $9.05_5 \pm 0.01_1$.

The CF_3^- anion has been the subject of comparatively few experimental studies. In a photodetachment study of CF_3^-, Brauman and co-workers[20] found a significant difference (ca. 0.8 eV) among the photodetachment threshold, the vertical detachment energy (VDE), and the adiabatic electron affinity (AEA) of CF_3, suggesting a significant change in geometry upon photodetachment. In a matrix-isolation study, Jacox et al.[15c] assigned two vibrational frequencies to CF_3^- in C_{3v} symmetry. Most empirical measurements[11,12] of the AEA of the CF_3 radical have been based on a dissociative electron attachment reaction or a thermochemical cycle involving the gas-phase acidity of trifluoromethane. No photoelectron spectrum of CF_3^- has been reported to date.

There have been several theoretical studies on the CF_3 radical and the CF_3^- anion.[21−26] The most detailed studies on the electron affinity have been published by Schaefer and co-workers,[27] Ricca,[9] and Dixon et al,[10] placing the adiabatic electron affinity at 1.78 ± 0.10 eV, 1.83 eV, and 1.77 ± 0.02 eV, respectively.

While information on the electron affinity and structural changes in photodetachment are contained in the photoelectron kinetic energy spectrum, measurements of photoelectron angular distributions (PADs) provide additional insights into photodetachment, such as the nature of the molecular orbital from which the photodetached electron originates and the dynamics of the photodetachment process.[28,29] Laboratory frame PADs are usually measured as a function of the angle, θ, between the electron recoil direction and the electric vector of linearly polarized light. The photoelectron angular distribution is represented by[28]

$$\frac{\partial\sigma}{\partial\Omega} = \frac{\sigma_{total}}{4\pi}[1 + \beta(E)P_2(\cos\theta)] \quad (1)$$

where σ_{total} is the total photodetachment cross section, $P_2(\cos\theta)$ is the second-order Legendre polynomial in $\cos\theta$, and $\beta(E)$ is the energy-dependent asymmetry parameter that can vary from −1 to 2. Laboratory PADs have been measured by a number of techniques over the last thirty years, ranging from recording the scattered intensity at a specific detection-laser-polarization angle[30] to the more recent application of photoelectron imaging

* Corresponding author. E-mail: rcontinetti@ucsd.edu.

10.1021/jp003137k CCC: $20.00
Published on Web 12/23/2000

techniques in the photoionization of neutral atoms[31] and neutral molecules[32,33] and the photodetachment of atomic negative ions.[34] In the experiments reported here, we have applied photoelectron imaging to the photodetachment of a molecular negative ion.

The objective of the present work is three-fold. First, we report the 4.80 eV laser photoelectron spectrum of CF_3^- and extract the adiabatic electron affinity of AEA[CF_3] = 1.82 ± 0.05 eV by a fit to the simulated Franck−Condon envelope of the photoelectron band. Second, we compare the experimentally determined electron affinity and derived heats of formation to the high-accuracy complete basis set (CBS-Q) method,[35] which purportedly predicts absolute heats of formation to within 0.77 kcal/mol after empirical "isodesmic bond additivity" corrections (BACs).[36] Finally, we report photoelectron images at a photon energy of 3.49 eV and determine the energy-averaged asymmetry parameter β describing the photoelectron angular distribution (PAD), and we interpret this in terms of the electronic structure of CF_3^-.

2. Experimental Section

The operation of the fast-ion-beam photoelectron spectrometer used in these experiments has been previously described in detail.[37,38] Trifluoromethyl anions are generated in a pulsed supersonic expansion at a repetition rate of 1 kHz by electron impact on a mixture of hexafluoroethane (~10%) in He/Ne (63%/27%) with a 1 keV electron beam. Anions are formed by secondary attachment processes and cooled by collisions in the jet expansion. The mass-selected beam of trifluoromethyl anions (m/e = 69) at an energy of 4 keV was crossed with the linearly polarized third harmonic (355 nm, 3.49 eV) of a Nd:YAG laser or the linearly polarized third harmonic (258 nm, 4.80 eV) of a Ti:Sapphire laser.

Measurement of the photoelectron spectrum at 258 nm was made using a large solid-angle fast-beam photoelectron spectrometer. With this spectrometer, the laboratory kinetic energy and recoil angle of the photodetached electrons are determined by time of flight and position of arrival using time- and position-sensitive photoelectron detectors.[37,38] The photoelectron spectrum at 4.80 eV was recorded with a resolution of ca. 5% $\Delta E_{fwhm}/E$ at 1.3 eV in a linear time-of-flight electron detector and was calibrated using the photodetachment of I^-.

In the photoelectron imaging experiment at 355 nm, a space-focusing electron optics assembly was used. This technique, developed by Hayden and co-workers,[39] permits the collection of the full 4πsr solid angle of the photodetached electrons. The design and implementation will be described in detail in a future publication.[40] Photodetachment occurs in an interaction volume with a small extraction field of 0.1 V/cm. Extracted photoelectrons pass through a grid, fly through a field free region, pass through a second grid, and are accelerated onto a time- and position-sensitive detector. As shown by Hayden and co-workers,[33] this configuration can be used to determine directly in three dimensions the energy and angular distributions of the photoelectrons. In the present experiments, however, the 0.5 ns timing resolution dictated that the angular distribution be extracted solely from the photoelectron image. The center-of-mass electron kinetic energy (eKE) resolution in the imaging configuration is ~12%$\Delta E_{fwhm}/E$. This spectrometer has been calibrated using the photodetachment of O^-. For the laser background to be reduced, both photoelectron spectra only include electrons which are counted in coincidence with a neutral particle of m/e = 69 (CF_3).

TABLE 1: Equilibrium Structures (in Å and deg) and Harmonic Vibrational Frequencies (in cm^{-1}) for Trifluoromethyl and Trifluoromethyl Anion[a]

	MP2(FC) 6-311+G(d)	CISD[b]	CEPA-1[c]	exp. (anharmonic)
		CF_3 (C_{3v})		
r_e(C−F)	1.319	1.315	1.3133	r_0 = 1.318 ± 0.02[d]
α_e(F−C−F)	111.3	111.3	111.32	α_0 = 110.7 ± 0.4[d]
θ_e	17.6	17.6	17.56	
ω1 (a_1)	1105 (1088)	1161	1114	1089 (gas)[e]
ω2 (a_1)	710 (699)	730	714	701 (gas)[f]
ω3 (e)	1271 (1251)	1387	1298	1260 (gas)[d]
ω4 (e)	516 (508)	520	518	509 (Ne)[g]
E_{tot}	−336.9582712	−336.775776	−	
				QCISD[g]
		CF_3^- (C_{3v})		
r_e(C−F)	1.432	1.419	1.436	
α_e (F−C−F)	99.9	99.8	99.8	
θ_e	27.9	27.9	28.0	
ω1 (a_1)	996 (981)	1046	980	1050 (Ne)[g]
ω2 (a_1)	617 (607)	650	609	
ω3 (e)	798 (789)	884	789	778 (Ne)[g]
ω4 (e)	454 (447)	467	449	
E_{tot}	−337.0123329	−336.830696	−	

[a] Scaled frequencies in parentheses (see text). Total electronic energies (E_{tot}) in Hartrees. [b] Ref 27. [c] Ref 25. [d] Ref 18. [e] Ref 17. [f] Ref 16. [g] Ref 15.

3. Computations

To aid in the analysis of our experimental data, we performed ab initio calculations on the CRAY J-90 supercomputer at the National Energy Research Supercomputer Center (NERSC) in Berkeley, using the GAUSSIAN 98 program package.[41] For the Franck−Condon analysis described below, the structures, harmonic frequencies, and force constants for CF_3 and CF_3^- were calculated at the MP2 level of theory, keeping the core electrons at the HF level (frozen core (FC)) using the 6-311+G(d) basis set and an unrestricted wave function for open-shell systems and a restricted wave function for closed-shell molecules. These calculations yielded good agreement for the geometric parameters and the vibrational frequencies when compared to available experimental data (Table 1).

To achieve high accuracy in the theoretical determination of the electron affinity (AEA) for CF_3, the vertical detachment energy (VDE) of CF_3^-, the inversion barriers of CF_3 and CF_3^-, and the heats of formation of CF_3 and CF_3^-, we used the CBS-Q protocol[35,36] implemented in GAUSSIAN 98.[41]. The mean absolute deviation for the heats of formation for a set of 76 organic species, including BACs, for this CBS-Q method has been determined to be 0.77 kcal/mol.[36] The details of the CBS-Q calculations can be obtained from the Supporting Information submitted with this article.

Franck−Condon factors (FCF) were calculated using the generating function method for a multidimensional harmonic oscillator, neglecting anharmonic effects.[42] The parallel mode approximation, in which it is assumed that the anionic ground state and the neutral ground state share normal coordinates, is often inappropriate for polyatomic molecules. Mode mixing induced by changes in geometry and the form of the normal modes between the ground state of the anion and the neutral species, called the Duschinsky effect,[43] must be taken into account. Chen and co-workers[1,4] developed the algorithm used to implement the generating function method for calculating Franck−Condon factors, including the Duschinsky effect, using the Cartesian displacement method. For a calculated geometry,

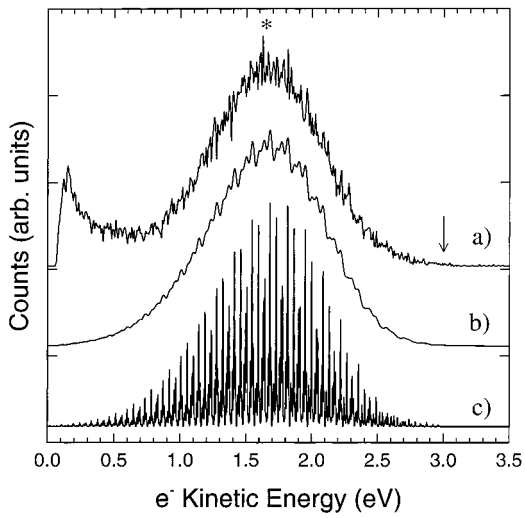

Figure 1. Photoelectron spectrum of CF_3^- collected at 258 nm (4.80 eV) (trace a). Electron kinetic energies are given in electronvolts (eV). Two simulated spectra, the stick spectrum (trace c) and the convoluted spectrum (trace b), are shown. The onset of the experimental spectrum is marked with an arrow, and the maximum in intensity is marked with an asterisk.

normal vibrational modes, frequencies, and reduced masses, Chen's code calculates the FCF intensity for each transition.[44] Transforming the calculated transition energy into the electronic kinetic energy yielded a stick spectrum that was convoluted with a Gaussian function in which the full-width half-maximum was chosen in order to simulate the experimental resolution ($\Delta E_{fwhm}/E \approx 5\%$) in the 4.80 eV photoelectron spectrum.

4. Results and Discussion

Figure 1a shows the photoelectron spectrum of CF_3^- recorded at a photon energy of 4.80 eV. In this spectrum, the electron kinetic energy, eKE, is related to the internal energy of the neutral and anion by the conservation of energy

$$\mathrm{eKE} = \mathrm{h}\nu - \mathrm{AEA} - E^0 + E^- \qquad (2)$$

In this equation, $h\nu$ is the photon energy, AEA is the adiabatic electron affinity, E^0 is the internal energy of the neutral, and E^- is the internal energy of the anion. In a prior study of the dissociation dynamics of ozone in this laboratory, Garner et al.[45] have shown cooling of O_3^- to a vibrational temperature of 450 K. For this temperature, most of the anions (~70%) are in their vibrational ground state. At the relatively high vibrational temperature of 450 K, however, sequence transitions from all the thermally populated vibrational levels will contribute to the band profile, even if the mode is not totally symmetric.[46,47]

The spectrum shown in Figure 1a was taken with the laser polarization perpendicular to the face of the electron detector, yielding a higher electron intensity than that in the polarization parallel to the face of the electron detector. This is a consequence of the anisotropic angular distribution of the photodetached electrons discussed in section 4.3. The spectrum directly yields the vertical detachment energy (VDE) for the neutral electronic state, using $\mathrm{VDE} = h\nu - \mathrm{eKE}_{max}$, where eKE_{max} is the electronic kinetic energy at the band maximum. This maximum is marked by an asterisk and was determined by a Gaussian fit to be $\mathrm{eKE}_{max} = 1.65$ eV, yielding a VDE of 3.15 eV. Determination of the AEA, the energy needed to form the ground electronic and vibrational state from the anion ground state, is complicated in the absence of a well-resolved vibrational structure. The arrow in Figure 1a indicates the onset of the photoelectron signal at 3.02 eV, yielding an adiabatic EA of 1.78 eV. The rising signal in the range eKE = 0−0.5 eV is due to laser background.

As shown below, there is a large change in the equilibrium geometry upon the photodetachment of CF_3^- ($\tilde{X}^1A_1$, C_{3v}) to CF_3 ($\tilde{X}^2A_1$, C_{3v}), which should induce significant Franck−Condon activity in the photoelectron spectrum. Therefore, another way of extracting the adiabatic electron affinity from the spectrum is by using a Franck−Condon simulation of the band profile. In a previous study of dichlorocarbene (CCl_2), Chen and coworkers[4] used a computed Franck−Condon envelope to deconvolute the partially resolved photoelectron spectrum and determined the adiabatic ionization potential and $\Delta H^0_{f,298}$of CCl_2. The force field in that study was harmonic and proved to be physically realistic enough to reproduce the observed band profile. Similarly, the simulation of the photoelectron spectrum of CF_3^- in the present work is done using ab initio potentials to extract the AEA from the spectrum. The simulated band profile is matched to the experimental spectrum, and an adiabatic electron affinity can be read from the fit, assuming that a match of both the intensity distribution and observed structure is achieved.

4.1. Deconvolution of the Spectrum. In Table 1, the results of ab initio calculations on the geometries and frequencies (MP2(FC)/6-311+G(d)) of CF_3^- ($\tilde{X}^1A_1$, C_{3v}) and CF_3 ($\tilde{X}^2A_1$, C_{3v}) are listed and compared to published theoretical and experimental data. The MP2 frequencies are scaled by a factor of 0.985 to match the available experimental gas-phase values in the neutral in a linear regression, similar to the approach of Pople et al.[48]

Examination of the structural parameters in Table 1 reveals that theory predicts CF_3^- and CF_3 to be pyramidal, in agreement with previous reports.[15,18] Furthermore, changes in both the bond distance $r_{e(C-F)}$ and the bond angle $\alpha_{e(F-C-F)}$ of −0.113 Å and +11.5°, respectively, are predicted upon photodetachment. There are only four normal modes in a symmetric AX_3 molecule: ν_1, the symmetric stretch (a_1); ν_2, the symmetric bend ("umbrella" mode, a_1); ν_3, the degenerate (e) asymmetric stretch; ν_4, the degenerate asymmetric bend (e). Transitions to all levels of totally symmetric vibrations in CF_3 (ν_1, ν_2) are allowed from the totally symmetric ground vibrational sate of CF_3^-, as are transitions to even quanta of the non-totally symmetric vibrations (ν_3, ν_4).[46,47] The frequencies of the non-totally symmetric modes ν_i (i = 3,4) change substantially between the negative ion and the neutral (see Table 1), so the sequence transitions, $\Delta v_i = 0$ from all the thermally populated low-frequency ν_3 and ν_4 levels in the anion will occur at an eKE offset from the fundamental transitions. Therefore, it was important to include these transitions in the simulation.

Similar to the isoelectronic molecules NF_3 and NF_3^+,[49] the potentials of both CF_3^- and CF_3[25] represent a double-well inversion potential, where the "umbrella" mode (ω_2) can be seen as the reaction coordinate for the inversion. The calculated classical barrier heights for inversion using the CBS-Q method are listed in Table 2 and compared to literature values. The inversion barrier in the anion is calculated to be 35 408 cm^{-1}, so no inversion splitting is expected at the bottom of the anion well. The inversion barrier in the neutral is calculated to be 9600 cm^{-1}, in agreement with published theoretical values (Table 2). A check of the potential surface of CF_3 using single point calculations at a series of geometries along the two a_1 coordinates showed that the potential is close to harmonic for up to 5 quanta in ω_2 and 10 quanta in ω_1.

TABLE 2: Calculated Inversion Barriers (cm^{-1}) for CF_3 and CF_3^-

method	barrier	ref
	CF_3	
CEPA-1	10295	25
DFT	8307	24
CISD	10082	22
MP4	10324	22
CBS-Q	9600	this work
	CF_3^-	
CBS-Q	35408	this work

TABLE 3: Adiabatic Electron Affinities (AEA in eV) and Vertical Detachment Energy (VDE in eV)

AEA	VDE	ref
	Experiment	
1.82 ± 0.05	3.13 ± 0.05	this work
1.84 ± 0.16	2.82 ± 0.01	11
	Theory	
1.76 ± 0.05	3.21 ± 0.05	this work
1.77 ± 0.02	–	10
1.83	–	9
1.78 ± 0.1	–	27

The Franck–Condon simulation in the harmonic approximation is shown in Figure 1c as a stick spectrum. The simulation includes transitions from the vibrational ground state of the anion to the totally symmetric vibrations in the neutral and the sequence bands for the asymmetric vibrations ν_i for $v'_i = 1 \leftarrow v''_i = 1$ (i = 3,4), consistent with the thermal distribution expected in these modes. In Figure 1b, the simulation is shown convoluted with an energy-dependent Gaussian function to simulate the resolution of the apparatus as previously discussed. In this spectrum, the partially resolved structure is reproduced well. A more sophisticated Franck–Condon analysis, which takes into account the double well potential of both the anion and the neutral and involves calculating the anharmonic vibrational term energies and wave functions, would be desirable, but it is beyond the scope of this paper.

Using the Franck–Condon simulation and matching the overall band contour rather than any single line gives the adiabatic electron affinity AEA[CF_3] = 1.82 ± 0.05 eV and a VDE of 3.13 ± 0.05 eV. We note that the largest calculated Franck–Condon factor, that for the $9\omega_1 + 2\omega_2$ transition (see Figure 1c), is a factor of 1500 larger than that for the origin. Shifting the simulated band contour to match the VDE of 3.15 eV determined by a direct Gaussian fit to the data does not reproduce the band profile at higher eKE as well. The band profile in this region is expected to be more accurate, since the neglected anharmonicity effects have a less significant effect on this branch of the spectrum. A conservative estimate for the uncertainty ($\pm$ 0.05 eV) of the AEA has been adopted for this reason.

Table 3 summarizes the experimental and calculated values for both the AEA and VDE compared to literature values. The value of AEA[CF_3] = 1.82 ± 0.05 eV obtained in this study compares well with the previously accepted experimental value[11] of AEA[CF_3] = 1.84 ± 0.16 eV and is in good agreement with the CBS-Q value presented here, AEA[CF_3] = 1.76 eV, and the computed values by Miller et al.,[27] Dixon et al.,[10] and Ricca.[9] The experimental value for the VDE [CF_3] = 3.13 ± 0.05 eV obtained in this study is 0.35 eV higher than the value extrapolated from photodetachment threshold measurements[20] but is in agreement with the computed value using the CBS-Q method of 3.21 eV.

4.2. Thermochemical Consequences and Comparison to CBS-Q Calculations. The heat of formation of the trifluoromethyl radical has been recently determined by Asher et al.[19] to be $\Delta H^0_{f,298}[CF_3] = -111.4 \pm 0.9$ kcal/mol. This value is 1 kcal/mol lower than the previously accepted values in the JANAF tables[50] and 1.4 kcal/mol higher than the Lias[11] value. For the trifluoromethyl anion, the literature value for the heat of formation is $\Delta H^0_{f,298}[CF_3^-] = -154.88 \pm 2.4$ kcal/mol in the stationary electron convention.[11] The stationary electron or ion convention does not account for the enthalpy of the attached electron at 298 K.[11] This assumption allows us a direct comparison of the experimental data in the ion convention to calculated ab initio values without correction for the additional electron in CF_3^-.

TABLE 4: Calculated and Experimental Heats of Formation $\Delta H^0_{f,298}$ in kcal/mol at 298 K and 1 Atm

	CF_3	CF_3^-	ref
	Experiment		
	–	-153.4 ± 1.5	this work
	-110.0 ± 1.0	-154.88 ± 2.4	11
	-112.4 ± 1.0	–	50
	-111.4 ± 0.9	–	19
	Theory		
CBS-Q + BAC	-112.1 ± 0.8	-152.6 ± 0.8	this work
	−111.2	−154.05	9
	−113.74	–	26

The heat of formation of CF_3^- is related to the heat of formation of CF_3 and the AEA of CF_3 as follows:

$$\Delta H^0_{f,298}[CF_3^-] = \Delta H^0_{f,298}[CF_3] - \mathrm{AEA}[CF_3] \qquad (3)$$

The AEA[CF_3] = 1.82 ± 0.05 eV extracted here by deconvolution of the photoelectron spectrum of CF_3^-, combined with the most recent value for $\Delta H^0_{f,298}[CF_3] = -111.4 \pm 0.9$ kcal/mol, yields $\Delta H^0_{f,298}[CF_3^-] = -153.4 \pm 1.5$ kcal/mol. This value is near the lower limit of the error bar of the previously determined value.

For comparison with these experimental results and as a test of the quoted accuracy of 0.77 kcal/mol for absolute thermochemical predictions using BAC corrections, CBS-Q calculations for both the CF_3 and CF_3^- were done. The results (Table 4), combined with the CBS-Q energies[36] and the heats of formation[50] of carbon and fluorine, give $\Delta H^0_{f,298}[CF_3] = -112.1$ kcal/mol and $\Delta H^0_{f,298}[CF_3^-] = -152.6$ kcal/mol after BAC. The predictions for both the radical and the anion are in excellent agreement with the presented results, providing another example of the application of the CBS-Q/BAC technique.

4.3. Photoelectron Image of CF_3^-. Figure 2 shows the photoelectron images recorded at 355 nm (3.49 eV) with the E vector of the polarized laser parallel (a) and perpendicular (b) to the face of the 2-D electron detector. In the present experiment, the laboratory coordinate system is defined by the direction of the ion beam along the y coordinate and the propagation of the laser beam along the x coordinate and the time-of-flight (TOF) (z coordinate) of the detached electrons.

The photoelectron image recorded with the E vector of the polarized laser parallel to the face of the electron detector (Figure 2a) shows an anisotropic electron angular distribution in the x and y coordinates and an isotropic distribution in the TOF (not shown). Rotating the laser polarization to point toward the detector shows that the photoelectron angular distribution is cylindrically symmetric about the electric vector of the laser (Figure 2b), as expected for electric-dipole photodetachment of a randomly oriented sample. The cylindrical symmetry allows us to deconvolve the image in Figure 2a using an Abel inversion. Figure 3 shows the angular distribution obtained using the

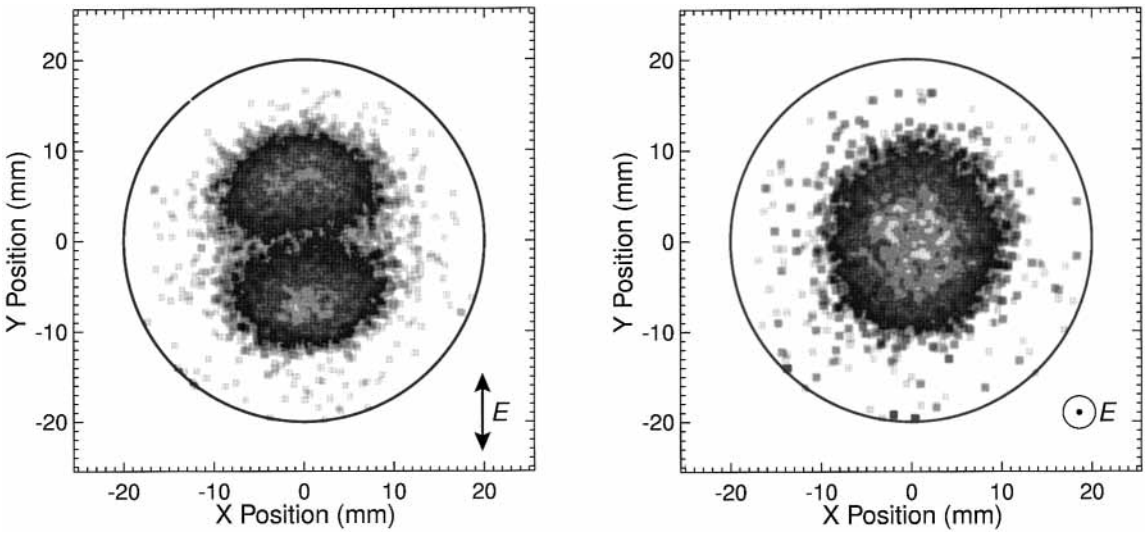

Figure 2. Photoelectron images of CF_3^- recorded at 355 nm (3.49 eV) with laser polarization parallel (a) and perpendicular (b) to the face of the electron detector. The images represent 256 × 256 pixels.

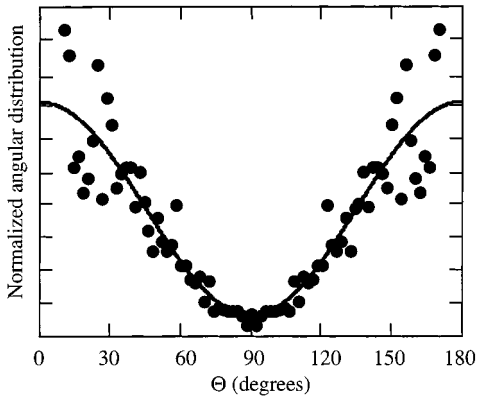

Figure 3. Photoelectron angular distribution (PAD) of CF_3^- obtained by Abel inversion for the photoelectron image in Figure 2a. Experimental data are shown by the filled circles, and the least-squares fit is shown by the solid line.

inverse Abel transform.[51−54] It is seen that the photoelectron angular distribution qualitatively follows a $\cos^2\theta$ distribution, with respect to the polarization of the detachment laser. The asymmetry parameter $\beta = 1.5 \pm 0.1$ has been extracted from the photoelectron angular distribution by fitting the data to eq 1 using a least-squares fit and is close to an ideal p wave photodetachment with a value of $\beta = 2.0$.

Brauman and co-workers developed an algorithm for the determination of the photodetachment cross section near threshold in the polyatomic case.[55] While their algorithm shows that s wave photodetachment is expected at threshold for photodetachment from the a_1 symmetry HOMO of CF_3^-, p wave photodetachment is also fully allowed by symmetry. As they pointed out, the selection rules only apply near threshold and cannot quantify the relative intensities of the allowed transitions. In the present experiment, the photon energy (355 nm; 3.49 eV) is 1.67 eV above the photodetachment threshold of 1.82 eV, so a dominant contribution from the allowed p wave photodetachment transition is not surprising.

5. Conclusions

We have recorded the photoelectron spectrum of CF_3^- at 4.80 and 3.49 eV and carried out ab initio calculations on both CF_3 and CF_3^-. From the 258 nm data and Franck−Condon simulations, we find that AEA[CF_3] = 1.82 ± 0.05 eV and VDE[CF_3^-] = 3.13 ± 0.05 eV, in good agreement with the calculated values of 1.76 and 3.21 eV, respectively, obtained using the CBS-Q method. From the experimentally known $\Delta H^0_{f,298}$ of the neutral CF_3, we derive $\Delta H^0_{f,298}[CF_3^-] = -153.4 \pm 1.5$ kcal/mol. CBS-Q calculations after "isodesmic bond additivity" corrections (BACs) yield excellent predictions of $\Delta H^0_{f,298}[CF_3^-]$ and $\Delta H^0_{f,298}[CF_3]$ within the quoted 0.77 kcal/mol accuracy for this correction. The photoelectron image of CF_3^- recorded at 355 nm shows an anisotropic angular distribution for the photodetached electrons with an anisotropy parameter of $\beta = 1.5 \pm 0.1$, consistent with photodetachment from an a_1 molecular orbital.

Acknowledgment. This work was supported by the U.S. Department of Energy (DOE) under Grant DE-FG03-908-ER14879. H.J.D. gratefully acknowledges partial support from a Forschungsstipendium sponsored by the Deutsche Forschungsgemeinschaft (DFG) and the DOE. L.S.A. is supported by a Cota Robles Fellowship and NSF Grant CHE-9700142. R.E.C. is a Camille Dreyfus Teacher-Scholar, an Alfred P. Sloan Research Fellow, and a Packard Fellow in Science and Engineering. We acknowledge T. Clements for useful discussions. We gratefully thank the National Energy Research Scientific Computing Center (NERSC) for providing computation time.

Supporting Information Available: Ab initio calculations at the CBS-Q level of theory. This material is available free of charge via the Internet at http://pubs.acs.org.

References and Notes

(1) Chen, P. In *Unimolecular and Bimolecular Reaction Dynamics*; Ng, C. Y., Baer, T., Powis, I., Eds.; Wiley: Chichester, 1994; pp 371−425 (and references therein).

(2) Robles, E. S. J.; Chen, P. *J. Phys. Chem.* **1994**, *98*, 6919.

(3) Gilbert, T.; Pfab, R.; Fischer, I.; Chen P. *J. Chem. Phys.* **2000**, *112*, 2575.

(4) Kohn, D. W.; Robles, E. S. J.; Logan, C. F.; Chen, P. *J. Phys. Chem.* **1993**, *97*, 4936.

(5) Alconcel, L. S.; Deyerl, H.-J.; Zengin, V.; Continetti, R. E. *J. Phys. Chem. A* **1999**, *103*, 9190.

(6) Ervin, K. M.; Lineberger, W. C. In *Advances in Gas-Phase Ion Chemistry*; Adams, N. G., Babcock, L. M., Eds.; JAI: Greenwich, 1992; Vol. 1, pp 121−166.

(7) *Chemical Kinetics of Small Radicals*; Alfassi, Z. B., Ed; CRC Press: Boca Raton, FL, 1988; Vol. 3, p 41.

(8) (a) Tsai, C.-P.; McFadden, D. L. *J. Phys. Chem.* **1989**, *93*, 2474. (b) Ryan, K. R.; Plumb, I. C. *J. Phys. Chem.* **1982**, *86*, 4678.
(9) Ricca, A. *J. Phys. Chem. A* **1999**, *103*, 1876.
(10) Dixon, D. A.; Feller, D.; Sandrone, G. *J. Phys. Chem. A* **1999**, *103*, 4744.
(11) Lias, S. G.; Bartmess, J. E.; Liebman, J. F.; Holmes, J. L.; Levin, R. D.; Mallard, W. G. *J. Phys. Chem. Ref. Data* **1988**, *17*, Suppl. 1.
(12) Christodoules, A. A.; McCorkle, D. L.; Christophorou, L. G. In *Electron Molecular Interaction and Their Application*; Christophorou, L. G., Ed.; Academic Press: New York, 1984; Vol. 2.
(13) Page, F. M.; Goode, G. C. *Negative Ions and the Magnetron*; Wiley: New York, 1969.
(14) Fessenden, R. W.; Schuler, R. H. *J. Chem. Phys.* **1965**, *43*, 2704.
(15) (a) Milligan, D. E.; Jacox, M. E.; Comeford, J. J. *J. Chem. Phys.* **1966**, *44*, 4058. (b) Milligan, D. E.; Jacox, M. E. *J. Chem. Phys.* **1968**, *48*, 2265. (c) Forney, D.; Jacox, M. E.; Irikura, K. K. *J. Chem. Phys.* **1994**, *101*, 8290.
(16) Carlson, G. A.; Pimentel, G. C. *J. Chem. Phys.* **1966**, *44*, 4053.
(17) Bozlee, B. J.; Nibler, J. W. *J. Chem. Phys.* **1986**, *84*, 3798.
(18) Yamada, C.; Hirota, E. *J. Chem. Phys.* **1983**, *78*, 1703.
(19) Asher, R. L.; Ruscic, B. *J. Chem. Phys.* **1997**, *106*, 210.
(20) Richardson, J. H.; Stephenson, L. M.; Brauman, J. I. *Chem. Phys. Lett.* **1975**, *30*, 17.
(21) Dixon, D. A. *J. Chem. Phys.* **1985**, *83*, 6055.
(22) Curtiss, L. A.; Pople, J. A. *Chem. Phys. Lett.* **1987**, *141*, 175.
(23) Dixon, D. A.; Fukunaga, T.; Smart, B. E. *J. Am. Chem. Soc.* **1986**, *108*, 4027.
(24) Gutsev, G. L. *Chem. Phys.* **1992**, *163*, 59.
(25) Horn, M.; Oswald, M.; Oswald, R.; Botschwina, P. *Ber. Bunsen-Ges. Phys. Chem.* **1995**, *99*, 323.
(26) Cheong, B. S.; Cho, H.-G. *J. Phys. Chem. A* **1997**, *101*, 7901.
(27) Miller, D. M.; Allen, W. D.; Schaefer, H. F. *Mol. Phys.* **1996**, *88*, 727.
(28) Cooper, J.; Zare, R. N. *J. Chem. Phys.* **1968**, *48*, 942.
(29) Chandra, N. *Chem. Phys.* **1986**, *108*, 301.
(30) Siegel, M. W.; Celotta, R. J.; Hall, J. L.; Levine, J.; Bennett, R. A. *Phys. Rev. A* **1972**, *6*, 607.
(31) Helm, H.; Bjerre, N.; Dyer, M. J.; Huestis D. L.; Saeed, M. *Phys Rev. Lett.* **1993**, *70*, 3221.
(32) Eppink, A T. J. B.; Parker, D. H. *Rev. Sci. Instrum.* **1997**, *68*, 3477.
(33) Davies, J. A.; Continetti, R. E.; Chandler, D. W.; Hayden C. C. *Phys Rev. Lett.* **2000**, *84*, 5983.
(34) Blondel, C.; Delsart, C.; Dulieu, F. *Phys. Rev. Lett.* **1996**, *77*, 3755.
(35) Ochterski, J. W.; Petersson, G. A.; Montgomery, J. A. *J. Chem. Phys.* **1996**, *104*, 2598.
(36) Petersson, G. A.; Malick, D. K.; Wilson, W. G.; Ochterski, J. W.; Montgomery, J. A.; Frisch, M. J. *J. Chem. Phys.* **1998**, *109*, 10570.
(37) Hanold, K. A.; Sherwood, C. R.; Garner, M. C.; Continetti, R. E. *Rev. Sci. Instrum.* **1995**, *66*, 5507.
(38) Hanold, K. A.; Luong, A. K.; Clements, T. G.; Continetti, R. E. *Rev. Sci. Instrum.* **1999**, *79*, 2270.
(39) Davies, J. A.; LeClaire, J. E.; Continetti, R. E.; Hayden, C. C. *J. Chem. Phys.* **1999**, *111*, 1.
(40) Alconcel, L. S.; Deyerl, H.-J.; Continetti, R. E. Manuscript in preparation.
(41) Frisch, M. J.; Trucks, G. W.; Schlegel, H. B.; Scuseria, G. E.; Robb, M. A.; Cheeseman, J. R.; Zakrzewski, V. G.; Montgomery, J. A.; Stratmann, R. E.; Burant, J. C.; Dapprich, S.; Millam, J. M.; Daniels, A. D.; Kudin, K. N.; Strain, M. C.; Farkas, O.; Tomasi, J.; Barone, V.; Cossi, M.; Cammi, R.; Mennucci, B.; Pomelli, C.; Adamo, C.; Clifford, S.; Ochterski, J.; Petersson, G. A.; Ayala, P. Y.; Cui, Q.; Morokuma, K.; Malick, D. K.; Rabuck, A. D.; Raghavachari, K.; Foresman, J. B.; Cioslowski, J.; Ortiz, J. V.; Stefanov, B. B.; Liu, G.; Liashenko, A.; Piskorz, P.; Komaromi, I.; Gomperts, R.; Martin, R. L.; Fox, D. J.; Keith, T.; Al-Laham, M. A.; Peng, C. Y.; Nanayakkara, A.; Gonzalez, C.; Challacombe, M.; Gill, P. M. W.; Johnson, B. G.; Chen, W.; Wong, M. W.; Andres, J. L.; Head-Gordon, M.; Replogle, E. S.; Pople, J. A. *GAUSSIAN 98* (Revision A.7); Gaussian, Inc.: Pittsburgh, PA, 1998.
(42) Warshel, A.; Karplus, M. *Chem. Phys. Lett.* **1972**, *17*, 7.
(43) Sharp, T. E.; Rosenstock, H. M. *J. Chem. Phys.* **1964**, *41*, 3453.
(44) We thank Prof. P. Chen for making this program available to us.
(45) Garner, M. C.; Hanold, K. A.; Resat, M. S.; Continetti, R. E. *J. Phys. Chem. A* **1997**, *101*, 6577.
(46) Herzberg, G. *Molecular Spectra and Molecular Structure III: Electronic Spectra and Electronic Structure of Polyatomic Molecules*; Krieger: Malabar, FL, 1991; pp 150−157.
(47) Weaver, A.; Arnold, D. W.; Bradforth, S. E.; Neumark D. M. *J. Chem. Phys.* **1991**, *94*, 1740.
(48) Pople, J. A.; Scott, A. P.; Wong, M. W.; Radom, L. *Isr. J. Chem.* **1993**, *33*, 345.
(49) Yates, B. F.; Schaefer, H. F. *J. Chem. Phys.* **1994**, *100*, 4459.
(50) Chase, M. W.; Davies, C. A.; Downey, J. R.; Frurip, D. J.; McDonald, R. A.; Syverud, A. N. *J. Phys. Chem. Ref. Data* **1985**, *14*, Suppl. 1 (JANAF Tables).
(51) Bordas, C.; Pauling, F.; Helm. H.; Huestis, D. L. *Rev. Sci. Instrum.* **1996**, *67*, 2257.
(52) Smith, L. M.; Keefer, D. R. *J. Quant. Spectrosc. Radiat. Transfer* **1988**, *39*, 367.
(53) Strickland, R. N.; Chandler, D. W. *Appl. Optics* **1991**, *30*, 1811.
(54) We thank Prof. T. N. Kitsopoulos for making this program available to us.
(55) Reed, K. J.; Zimmermann, A. H.; Andersen, H. C.; Brauman, J. I. *J. Chem. Phys.* **1976**, *64*, 1368.